Hydrol. Earth Syst. Sci. Discuss., 12, 11269–11289, 2015
www.hydrol-earth-syst-sci-discuss.net/12/11269/2015/
doi:10.5194/hessd-12-11269-2015

Hydrology and Earth System Sciences
Discussions
Open Access

Synchrony of trend shifts in Sahel summer rainfall and global oceanic evaporation, 1950–2012

A. Diawara[1], Y. Tachibana[1], K. Oshima[2], H. Nishikawa[1], and Y. Ando[1]

[1]Weather and Climate Dynamics Division, Mie University, Tsu, Japan
[2]Institute of Arctic Climate and Environment Research, Japan Agency for Marine-Earth Science and Technology, Yokosuka, Japan

Received: 2 September 2015 – Accepted: 13 October 2015 – Published: 2 November 2015

Correspondence to: Y. Tachibana (tachi@bio.mie-u.ac.jp)

Published by Copernicus Publications on behalf of the European Geosciences Union.

Abstract

Between 1950 and 2012, summer (rainy season) rainfall in the Sahel changed from a multi-decadal decreasing trend to an increasing trend (positive trend shift) in the mid-1980s. We found that this trend shift was synchronous with similar trend shifts in global oceanic evaporation and in land precipitation in all continents except the Americas. The trend shift in oceanic evaporation occurred mainly in the Southern Hemisphere (SH) and the subtropical oceans of the Northern Hemisphere (NH). Because increased oceanic evaporation strengthens the atmospheric moisture transport toward land areas, the synchrony of oceanic evaporation and land precipitation is reasonable. Surface scalar winds over the SH oceans also displayed a positive trend shift. Sea surface temperature (SST) displayed a trend shift in the mid-1980s that was negative (increasing, then decreasing) in the SH and positive in the NH. Although SST had opposite trend shifts in both hemispheres, the trend shift in evaporation was positive in both hemispheres. We infer that because strong winds promote evaporative cooling, the trend shift in SH winds strengthened the trend shifts of both SST and evaporation in the SH. Because high SST promotes evaporation, the trend shift in NH SST strengthened the NH trend shift in evaporation. Thus differing oceanic roles in the SH and NH generated the positive trend shift in evaporation; however, the details of moisture transport toward the Sahel are still unclear.

1 Introduction

The Sahel region, the area of western Africa between 10 and 20° N, commonly suffers from severe drought and is synonymous with unstable climate (Dai, 2011). Many studies have shown that rainfall varies greatly in the Sahel. Folland et al. (1986) established a relationship between Sahel rainfall and hemispheric disparity in sea surface temperature (SST) on multi-decadal time scales, such that when SST is higher (lower) than normal in the Southern Hemisphere (SH) and lower (higher) than normal in the

Northern Hemisphere (NH), the Sahel is drier (wetter) than normal. Several studies have shown that the Indian Ocean, the North and South Atlantic, the SH oceans and the Mediterranean Sea have, alone or together, some kind of remote influence on the distribution of Sahel rainfall (Palmer, 1986; Giannini et al., 2003; Wolter, 1989; Janicot et al., 1996; Rowell, 2003; Hagos and Cook, 2008; Diatta and Fink, 2014). Munemoto and Tachibana (2012), using updated datasets, confirmed the relationship of Folland et al. (1986) and also showed that correspond to the more recent pattern of Sahel rainfall, which shifted from a decreasing trend to an increasing trend in the mid-1980s.

Although long-term climate trends are generally related to the state of the ocean, the exact linkage between the multi-decadal variation of Sahel rainfall and the global ocean is unclear. Understanding the source of Sahel rainfall should help in explaining its variation. The global hydrological cycle comprises evaporation from the ocean surface and transport of water vapour over the continents. It is reasonable that moisture transport from different parts of the world ocean may have some effects, either singly or in combination, on precipitation over Africa and the Sahel in particular. In this study, we analysed datasets of global-scale evaporation for the second half of the 20th century in an effort to demonstrate the relationship of the shift in Sahel rainfall to shifts in oceanic evaporation. We also sought insight into the causes of long-term variations in global oceanic evaporation.

2 Data and methods

For precipitation on land, we used monthly data from 1949 to 2014 in the National Oceanic and Atmospheric Administration (NOAA) Precipitation Reconstruction over Land (PREC/L) database (Chen et al., 2002) with a spatial resolution of 1.0° in latitude and longitude. For SST, we used monthly data from 1953 to 2012 in the NOAA Extended Reconstructed SST Version 3 (NOAA ERSST V3) dataset, which is constructed from SST data in the International Comprehensive Ocean-Atmosphere Data Set (ICOADS) (Smith et al., 2007; Xue et al., 2003). Monthly 10 m scalar wind speed data from 1950 to 2011 came from Wave and Anemometer-based Sea Surface Wind (WASWind) version 1.0.1 (Tokinaga and Xie, 2011), derived from ship observations in ICOADS and presented at a resolution of $4^{\circ} \times 4^{\circ}$. Specific humidity data at 2-degree resolution was from ICOADS. Both wind speed and specific humidity databases have missing values in areas outside shipping routes, especially in high latitudes. We used latent heat flux (LHF) data for 1950–2012 from the National Centers for Environmental Prediction/National Center for Atmospheric Research (NCEP/NCAR) Reanalysis (Kalnay et al., 1996) as a robust proxy for evaporation from the ocean. We also used data from the Japanese Re-Analysis 55 Years (JRA-55) (Kobayashi et al., 2015) and the European Centre for Medium-Range Weather Forecasts (ECMWF) 40-year Reanalysis (ERA-40) (Uppala et al., 2005) for comparison with the LHF data from NCEP/NCAR to address possible reliability problems in moisture data from the pre-satellite era. Although there are some differences among these three databases, the differences do not significantly influence our conclusions. Our analysis used mainly July-August-September (JAS) averages, corresponding to the rainy season in the Sahel region.

Figure 1 shows the long-term (1950–2012) value of JAS average precipitation in northern Africa. Our study area, defined as the region bounded by 10 and 20° N and 8° W and 30° E, was chosen to avoid coastal influences on seasonal rainfall in the Sahel. Figure 2 shows the variation of JAS average rainfall in the study area from 1950 through 2012. Sahel rainfall followed a decreasing trend from the early 1960s to the mid-1980s, followed by an increasing trend for the rest of the study period. The driest year of the study period was 1984 (Munemoto and Tachibana, 2012). The mid-1980s mark a clear reversal in these multi-decadal trends. The signature of this trend shift is not sensitive to the definition of the study area (results not shown).

In assessing the degree to which trends in other climatic parameters are synchronized with the Sahel trend shift, we divided the time series of all datasets into the subperiods 1950–1984 and 1985–2012. We defined the trend in each subperiod as the angle of inclination, $\tan\theta$, of the time series, as calculated from the linear regression

HESSD
12, 11269–11289, 2015

coefficient using the least squares method. We defined the strength of the trend shift, $\delta \tan\theta$, as $\tan\theta_2 - \tan\theta_1$, where the subscripts 1 and 2 denote the subperiods before and after 1984, respectively. To confirm that the trends of the two subperiods differed in sign, we added the condition $\tan\theta_1 \cdot \tan\theta_2 < 0$. We named decreasing to increasing (increasing to decreasing) trend shift as positive (negative) trend shift, i.e. $\delta \tan\theta > 0$ ($\delta \tan\theta < 0$) and $\tan\theta_1 \cdot \tan\theta_2 < 0$.

3 Results

3.1 Trend shifts of Sahel precipitation and ocean evaporation

The time series of global JAS mean LHF displays a decreasing trend before the mid-1980s, followed by an increase (Fig. 2). Although this increase ceased after the mid-1990s, the turning point of the trend shift coincided with that of Sahel rainfall. Global annual mean LHF also had similar trend shift to those of the JAS mean (figure not shown). This synchrony suggests that at the multi-decadal time scale, the variability of Sahel rainfall may be physically linked to transport of the moisture evaporated from the oceans. We also investigated global mean sensible heat flux but found no significant trends during the study period.

The trend shift of LHF in the world ocean may be related to precipitation in and outside the Sahel. The results of our investigation of this possibility are shown for both JAS and annual precipitation in Fig. 3. The trend shift over the Sahel is stronger for annual precipitation than for JAS precipitation. The areas where the positive trend shift (from decreasing to increasing) in JAS precipitation is large are the Sahel, western coastal areas of South Asia, and equatorial South America (Fig. 3a).

For annual precipitation, areas of positive trend shift exceed areas of negative trend shift (Fig. 3b). Positive trend shifts are particularly strong in the Sahel, western coastal areas of South Asia, and southern Chile, and less strong in Korea, Japan, the Philippines, Alaska, and northern Eurasia. Negative trend shifts are seen in South America,

HESSD
12, 11269–11289, 2015

most of the Southern Hemisphere, most of North America, and inland Eurasia. Areas of negative trend shift are weaker and narrower than areas of positive trend shift. These results indicate that a positive trend shift in precipitation occurred not only in the Sahel but elsewhere on the globe.

3.2 Global SST trend shift

Sahel rainfall is known to be related to nearby SST (Lough, 1986; Bader and Latif, 2003; Chung and Ramanathan, 2006) and remote SST (Folland et al., 1986; Janicot et al., 1996; Rowell, 2003; Fontaine et al., 2011; Munemoto and Tachibana, 2012; Diatta and Fink, 2014). Figure 4 shows that areas of positive trend shift in JAS SST over the oceans are widespread in the NH, meaning that SST decreased until 1984 and then increased. Areas of negative trend shift are mostly in the SH, particularly the eastern tropical Pacific and the South Atlantic Ocean. The obvious contrast between hemispheres suggests that the change in JAS Sahel rainfall is somehow related to the hemispheric contrast in SST. These results are consistent with the findings of Folland et al. (1986) and Munemoto and Tachibana (2012).

3.3 Trend shift of global ocean evaporation

Figure 5 shows the geographic distribution of the trend shift in mean JAS ocean evaporation, as signified by LHF. The areas of negative shift are much narrower than those of positive shift. A positive trend shift occupies the whole latitude range from 60° S to 40° N, except in the western South Pacific, northern and western Indian Ocean, and the Caribbean Sea. Areas where the trends changed sign between subperiods ($\tan\theta_1 \cdot \tan\theta_2 < 0$) cover most of the oceans, suggesting that the trend shift was genuine and worldwide.

HESSD
12, 11269–11289, 2015

3.4 Trend shifts of wind, humidity

Latent heat flux is determined by surface wind speed and the humidity deficit over the ocean. Figure 6 shows the trend shift of JAS surface scalar wind speeds over the ocean. This shift is positive over most of the SH, particularly in the eastern Pacific Ocean. Many of these positive areas match areas of positive trend shift in LHF (Fig. 5). In the NH, the trend shift is positive over the subtropical central and eastern Pacific. Over the western subtropical North Atlantic ocean, the trend shift in the scalar wind is not in agreement with the trend shift in LHF. However, the overall similarity of Figs. 5 and 6 signifies that trend shifts in wind speed over the ocean partially account for the trend shift in LHF.

The trend shift in the JAS deficit of surface specific humidity, as determined from its saturated value at the local SST, is shown in Fig. 7. The geographic distribution of this positive trend shift is essentially global, similar to those of SST (Fig. 4) and LHF (Fig. 5) in the NH and the southern Pacific Ocean. The positive trend shift of global evaporation from the ocean is therefore also partially explained by this trend shift.

4 Discussion and conclusion

Our study demonstrates that the shift in the trend of JAS Sahel rainfall from decrease to increase (positive trend shift) that occurred in the mid-1980s coincided with shifts in global-scale SST and evaporation from the oceans (Table 1). The Sahel constitutes the world's largest area in which this trend shift occurred. We found that the Sahel trend shift was synchronous with similar positive trend shifts in global oceanic evaporation (Fig. 2) and in land precipitation outside the Sahel, except in the Americas (Fig. 3). In detail, the trend shift in oceanic evaporation (as indicated by LHF) encompassed the SH and the subtropical NH, including the Pacific, Atlantic, and Indian Oceans (Fig. 5). Because increased oceanic evaporation strengthens global moisture transport toward the land, the synchronization of these trend shifts is physically plausible, and indeed the area of increased LHF exceeded the area of decreased LHF. Trend shifts also occurred in the mid-1980s in SST: the shift was negative (increase to decrease) in the SH and positive in the NH, giving rise to an interhemispheric contrast in SST (Fig. 4). The surface scalar wind over the ocean had a positive trend shift, mainly in the SH, that extended to the subtropical Pacific Ocean in the NH (Fig. 6). The humidity deficit displayed a positive trend shift in both hemispheres, particularly in the Pacific Ocean (Fig. 7).

From these results, we can suggest possible processes that connect the trend shifts of the global oceans and Sahel rainfall (Fig. 8). The main reason for the positive trend shift in LHF is the positive trend shift in scalar wind, particularly in the SH, because surface wind promotes evaporation from the ocean. In general, high LHF lowers the SST due to evaporative cooling. Therefore, the negative trend shift in SST in the SH may be an effect of the positive trend shift in the scalar wind.

In the NH at latitudes lower than 40° N, the LHF trend shift tended to be positive, in synchrony with the positive SST trend shift. Because high SST in low latitudes generally promotes evaporation, the positive trend shift in LHF may be a consequence of the positive trend shift in SST. The positive trend shift in the humidity deficit in the NH also supports this inference. Thus, the positive SST trend shift in the NH may be linked to the positive LHF trend shift. Although the trend shift in SST is positive in the NH and negative in the SH, hemispheric differences in the role of SST may result in a global positive trend shift in LHF.

Our study offers an explanation for these global-scale trend shifts; however, the reason for the outsized signature of Sahel rainfall is still problematic. Many previous studies have argued for the influence of SST in different remote sites (Folland et al., 1986; Czaja and Frankignoul, 2002; Dijkstra, 2006; Ting et al., 2009), including the Atlantic Ocean (Hu and Huang, 2006; Marullo et al., 2011; Martin et al., 2014), Pacific Ocean (Rowntree, 1972; Pan and Oort, 1983; Cayan and Peterson, 1989; Wallace et al., 1989), and Indian Ocean (Clemens et al., 1991; Ashok et al., 2001, 2003; Annamalai et al., 2005). Probably there is no single determining influence. To identify how evaporation in these remote oceans drives Sahel rainfall, idealized atmospheric general circulation model studies will need to incorporate the anomalous SST patterns shown in this study. The processes underlying the trend shift of the ocean surface wind also must be identified. Also of interest is how the trend shift in oceanic evaporation might affect the global salinity distribution, and in turn the global thermohaline circulation.

Acknowledgements. We thank the Ministry of Education, Culture, Sports, Science and Technology (MEXT) for the opportunity afforded by the international student scholarship program. MEXT supported this study through a Grant-in-Aid for Scientific Research on Innovative Areas (Grant Number 22106003). We extend special thanks to Kunihiko Kodera and Koji Yamazaki for insightful discussions. The Grid Analysis and Display System (GrADS) and Generic Mapping Tools (GMT) were used to draw the figures. The SST NOAA_ERSST_V3 data, the precipitation PREC/L and the latent heat flux are provided by the NOAA/OAR/ESRL PSD, Boulder, Colorado, USA, from their Website at http://www.esrl.noaa.gov/psd/, the WASWind data and the specific humidity are from ICOADS at https://climatedataguide.ucar.edu/climate-data/waswind-wave-and-anemometer-based-sea-surface-wind.

References

Annamalai, H., Liu, P., and Xie, S. P.: Southwest Indian Ocean SST Variability Its Local Effect and Remote Influence on Asian Monsoons, J. Climate, 18, 4150–4167, doi:10.1175/JCLI3533.1, 2005.

Ashok, K., Guan, Z., and Yamagata, T.: Impact of the Indian Ocean dipole on the relationship between the Indian Monsoon rainfall and ENSO, Geophys. Res. Lett., 28, 4499–4502, doi:10.1029/2001GL013294, 2001.

Ashok, K., Guan, Z., and Yamagata, T.: Influence of the Indian Ocean Dipole on the Australian winter rainfall, Geophys. Res. Lett., 30, 1821–1825, doi:10.1029/2003GL017926, 2003.

Bader, J. and Latif, M.: The impact of decadal-scale Indian Ocean sea surface temperature anomalies on Sahelian rainfall and the North Atlantic Oscillation, Geophys. Res. Lett., 30, 2169–2172, doi:10.1029/2003GL018426, 2003.

Cayan, D. R. and Peterson, D. H.: The Influence of North Pacific Atmospheric Circulation on Streamflow in the West, in: Aspects of Climate Variability in the Pacific and the Western Americas, Geophys. Monogr. No. 55, Amer. Geophys. Union, Washington, D. C., 375–397, doi:10.1029/GM055p0375, 1989.

Chen, M., Xie, P., Janowiak, J. E., and Arkin, P. A.: Global Land Precipitation: A 50-yr Monthly Analysis Based on Gauge Observations, J. Hydrometeorol., 3, 249–266, 2002.

Chung, C. E. and Ramanathan, V.: Weakening of North Indian SST Gradients and the Monsoon Rainfall in India and the Sahel, J. Climate, 19, 2036–2045, doi:10.1175/JCLI3820.1, 2006.

Clemens, S., Prell, W., Murray, D., Shimmield, G., and Weedon, G.: Forcing mechanisms of the Indian Ocean monsoon, Nature, 353, 720–725, doi:10.1038/353720a0, 1991.

Czaja, A. and Frankignoul, C.: Observed Impact of Atlantic SST Anomalies on the North Atlantic Oscillation, J. Climate, 15, 606–623, doi:10.1029/2004JD005676, 2002.

Dai, A.: Drought under global warming: a review, WIREs Climate Change, 2, 45–65, doi:10.1002/wcc.81, 2011.

Diatta, S. and Fink, A. H.: Statistical relationship between remote climate indices and West African monsoon variability, Int. J. Climatol., 34, 3348–3367, doi:10.1002/joc.3912, 2014.

Dijkstra, H. A.: Interaction of SST Modes in the North Atlantic Ocean, J. Phys. Oceanogr., 36, 286–299, doi:10.1175/JPO2851.1, 2006.

Folland, C. K., Palmer, T. N., and Parker, D. E.: Sahel rainfall and worldwide sea temperatures, 1901–85, Nature, 320, 602–607, doi:10.1038/320602a0, 1986.

Fontaine, B., Gaetani, M., Ullmann, A., and Roucou, P.: Time evolution of observed July–September sea surface temperature-Sahel climate teleconnection with removed quasi-global effect (1900–2008), J. Geophys. Res., 116, D04105, doi:10.1029/2010JD014843, 2011.

Giannini, A., Saravanan, R., and Chang, P.: Oceanic forcing of Sahel rainfall on annually to interdecadal time scales, Science, 302, 1027–1030, doi:10.1126/science.1089357, 2003.

Hagos, S. M. and Cook, K. H.: Ocean Warming and Late-Twentieth-Century Sahel Drought and Recovery, J. Climate, 21, 3797–3814, doi:10.1175/2008JCLI2055.1, 2008.

Hu, Z. Z. and Huang, B.: Physical Processes Associated with the Tropical Atlantic SST Meridional Gradient, J. Climate, 19, 5500–5518, doi:10.1175/JCLI3923.1, 2006.

Janicot, S., Moron, V., and Fontaine, B.: Sahel droughts and ENSO dynamics, Geophys. Res. Lett., 23, 515–518, doi:10.1029/96GL00246, 1996.

Kalnay, E., Kanamitsu, M., Kistler, R., Collins, W., Deaven, D., Gandin, L., Iredell, M., Saha, S., White, G., Woollen, J., Zhu, Y., Cheillab, M., Ebsuzaki, W., Higgins, W., Janowiak, J., Mo,

HESSD
12, 11269–11289, 2015

Synchrony of trend shifts in Sahel summer rainfall and global oceanic evaporation

A. Diawara et al.

K. C., Ropelewski, C., Wang, J., Leetma, A., Reynolds, P., Jenne, R., and Joseph, D.: The NCEP/NCAP 40-year reanalysis project, B. Am. Meteorol. Soc., 77, 437–470, 1996.

Kobayashi, S., Ota, Y., Harada, Y., Ebita, A., Moriya, M., Onoda, H., Onogi, K., Kamahori, H., Kobayashi, C., Endo, H., Miyaoka, K., and Takahashi, K.: The JRA-55 Reanalysis: General Specifications and Basic Characteristics, J. Meteorol. Soc. Jpn., 93, 5–48, doi:10.2151/jmsj.2015-001, 2015.

Lough, J. M.: Tropical Atlantic Sea Surface Temperatures and Rainfall Variations in Subsaharan Africa, Mon. Weather. Rev., 114, 561–570, doi:10.1175/1520-0493(1986)114<0561:TASSTA>2.0.CO;2, 1986.

Martin, E. R., Thorncroft, C., and Booth, B. B.: The Multidecadal Atlantic SST – Sahel Rainfall Teleconnection in CMIP5 Simulations, J. Climate, 27, 784–806, doi:10.1175/JCLI-D-13-00242.1, 2014.

Marullo, S., Artale, V., and Santoleri, R.: The SST Multidecadal Variability in the Atlantic–Mediterranean Region and Its Relation to AMO, J. Climate, 24, 4385–4401, doi:10.1175/2011JCLI3884.1, 2011.

Munemoto, M. and Tachibana, Y.: The recent trend of increasing precipitation in Sahel and the associated inter-hemispheric dipole of global SST, Int. J. Climatol., 32, 1346–1353, doi:10.1002/joc.2356, 2012.

Palmer, T. N.: Influence of the Atlantic, Pacific and Indian Oceans on Sahel rainfall, Nature, 322, 251–253, doi:10.1038/322251a0, 1986.

Pan, Y. H. and Oort, A. H.: Global Climate Variations Connected with Sea Surface Temperature Anomalies in the Eastern Equatorial Pacific Ocean for the 1958–73 Period, Mon. Weather. Rev., 111, 1244–1258, doi:10.1175/1520-0493(1983)111<1244:GCVCWS>2.0.CO;2, 1983.

Rowell, D. P.: The Impact of Mediterranean SSTs on the Sahelian Rainfall Season, J. Climate, 16, 849–862, doi:10.1175/1520-0442(2003)016<0849:TIOMSO>2.0.CO;2, 2003.

Rowntree, P. R.: The influence of tropical east Pacific Ocean temperatures on the atmosphere, Q. J. Roy. Meteorol. Soc., 98, 290–321, doi:10.1002/qj.49709841605, 1972.

Smith, T. M., Reynolds, R. W., Peterson, T. C., and Lawrimore, J.: Improvements to NOAA's Historical Merged Land-Ocean Surface Temperature Analysis (1880–2006), J. Climate, 21, 2283–2296, 2008.

Ting, M., Kushnir, Y., Seager, R., and Li, C.: Forced and Internal Twentieth-Century SST Trends in the North Atlantic, J. Climate, 22, 1469–1481, doi:10.1175/2008JCLI2561.1, 2009.

HESSD

12, 11269–11289, 2015

Title Page

Abstract | Introduction

Conclusions | References

Tables | Figures

◂◂ | ▸▸

◂ | ▸

Back | Close

Full Screen / Esc

Printer-friendly Version

Interactive Discussion

Tokinaga, H. and Xie, S. P.: Wave and Anemometer-based Sea Surface Wind (WASWind) for Climate Change Analysis, J. Climate, 24, 267–285, doi:10.1175/2010JCLI3789.1, 2011.

Uppala, S. M.: The ERA-40 re-analysis, Q. J. Roy. Meteorol. Soc., 131, 2961–3012, doi:10.1256/qj.04.176, 2005.

Wallace, J. M., Mitchell, T. P., and Deser, C.: The Influence of Sea-Surface Temperature on Surface Wind in the Eastern Equatorial Pacific: Seasonal and Interannual Variability, J. Climate, 2, 1492–1499, doi:10.1175/1520-0442(1989)002<1492:TIOSST>2.0.CO;2, 1989.

Wolter, K.: Modes of tropical circulation, Southern Oscillation, and Sahel rainfall anomalies, J. Climate, 2, 149-172, doi:10.1175/1520-0442(1989)002<0149:MOTCSO>2.0.CO;2, 1989.

Xue, Y., Smith, T. M., and Reynolds, R. W.: Interdecadal changes of 30-yr SST normals during 1871–2000, J. Climate, 16, 1601–1612, doi:10.1175/1520-0442-16.10.1601, 2003.

HESSD

12, 11269–11289, 2015

Synchrony of trend shifts in Sahel summer rainfall and global oceanic evaporation

A. Diawara et al.

Table 1. Summary of Results for JAS Meteorological Parameters. "Positive" indicates that a shift from decrease to increase occurred during 1950 to 2012; "negative" indicates a shift from increase to decrease.

	Sahel rain	SST	LHF	Wind	Humidity deficit
Northern Hemisphere	Positive	Positive	Positive	Positive (tropical Pacific)	Positive
Southern Hemisphere		Negative	Positive	Positive	Positive (Pacific)

Discussion Paper | Discussion Paper | Discussion Paper | Discussion Paper |

HESSD

12, 11269–11289, 2015

Synchrony of trend shifts in Sahel summer rainfall and global oceanic evaporation

A. Diawara et al.

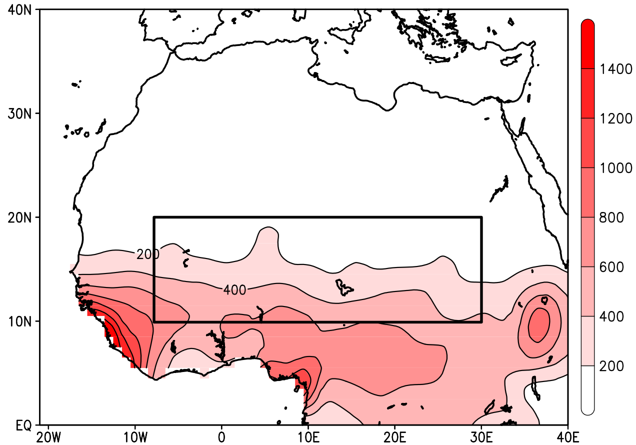

Figure 1. Long-term (1950–2012) mean summer (JAS) rainfall in northern Africa. The study area defined as the Sahel region is outlined in black. The unit is mm.

HESSD
12, 11269–11289, 2015

Synchrony of trend shifts in Sahel summer rainfall and global oceanic evaporation

A. Diawara et al.

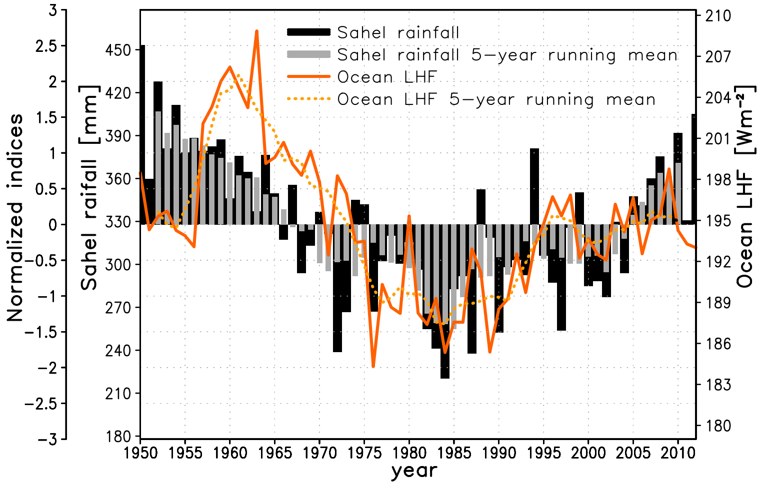

Figure 2. Time series of JAS Sahel rainfall (mm) and mean LHF (W m^{-2}) from oceans from 1950 to 2012.

HESSD
12, 11269–11289, 2015

Synchrony of trend shifts in Sahel summer rainfall and global oceanic evaporation

A. Diawara et al.

Title Page
Abstract | Introduction
Conclusions | References
Tables | Figures
◂ | ▸
Back | Close
Full Screen / Esc
Printer-friendly Version
Interactive Discussion

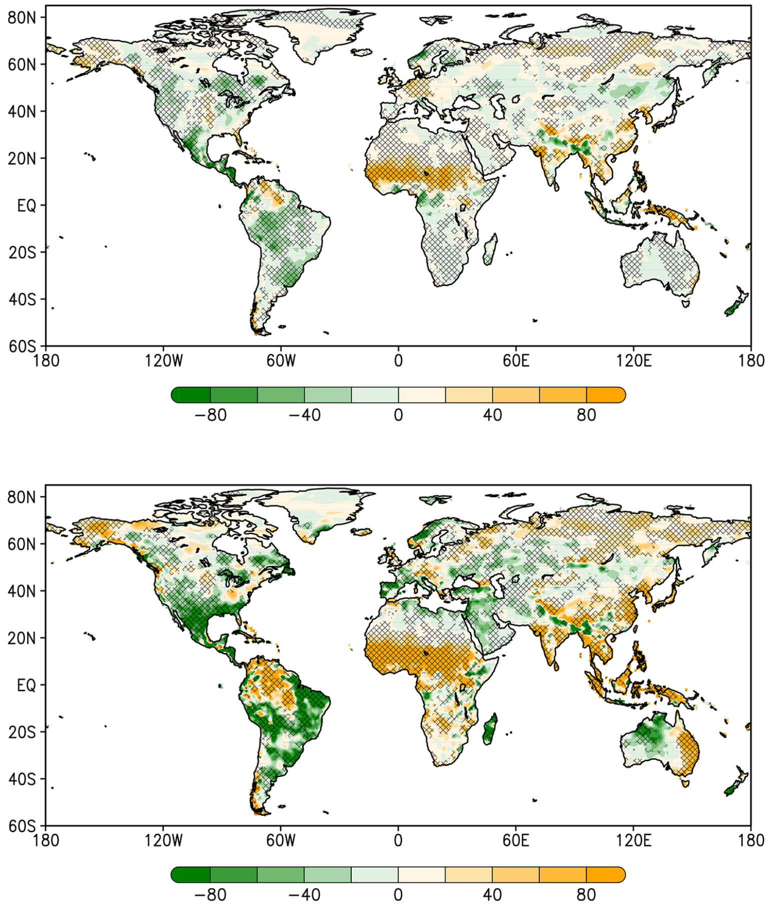

Figure 3. Global maps of the trend shift for **(a)** JAS precipitation (mm 10 years^{-1}) and **(b)** annual precipitation. Shading denotes $\delta \tan \theta$. Hatching represents areas where trends changed sign between the two parts of the study period ($\tan \theta_1 \cdot \tan \theta_2 < 0$).

HESSD
12, 11269–11289, 2015

Synchrony of trend shifts in Sahel summer rainfall and global oceanic evaporation

A. Diawara et al.

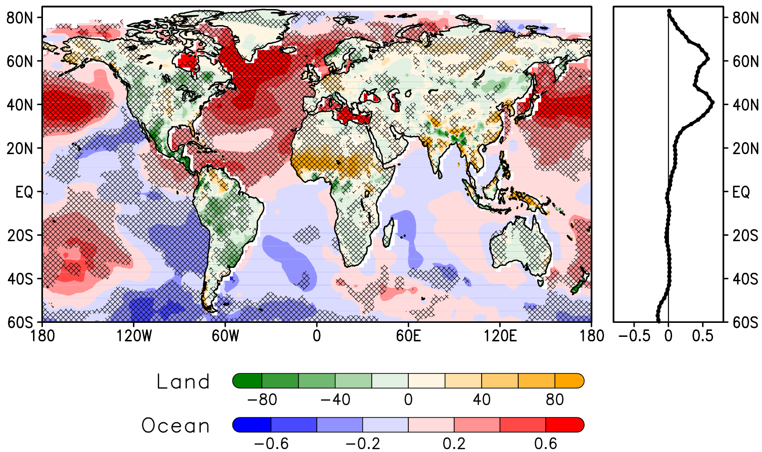

Figure 4. Left panel: trend shifts in SST ($K\,10\,years^{-1}$) and right panel: latitude profile of its zonal mean. Land areas display trend shifts in JAS precipitation from Fig. 3a.

HESSD
12, 11269–11289, 2015

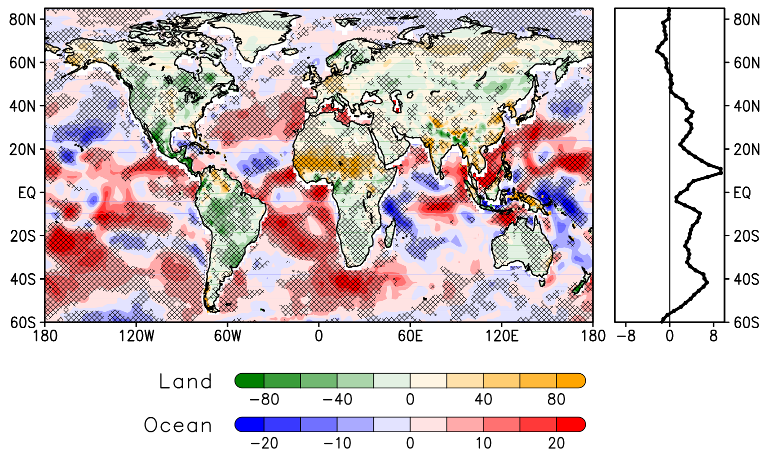

Figure 5. Left panel: trend shifts in latent heat flux ($W\,m^{-2}$ 10 $years^{-1}$) and right panel: latitude profile of its zonal mean. Land areas display trend shifts in JAS precipitation from Fig. 3a.

HESSD
12, 11269–11289, 2015

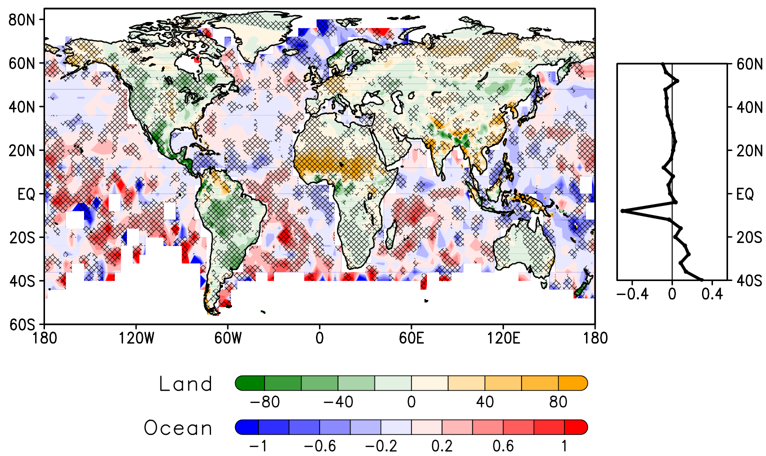

Figure 6. Left panel: trend shifts in scalar wind speed over the ocean ($m\,s^{-1}$ 10 $years^{-1}$) and right panel: latitude profile of its zonal mean. Land areas display trend shifts in JAS precipitation from Fig. 3a.

HESSD
12, 11269–11289, 2015

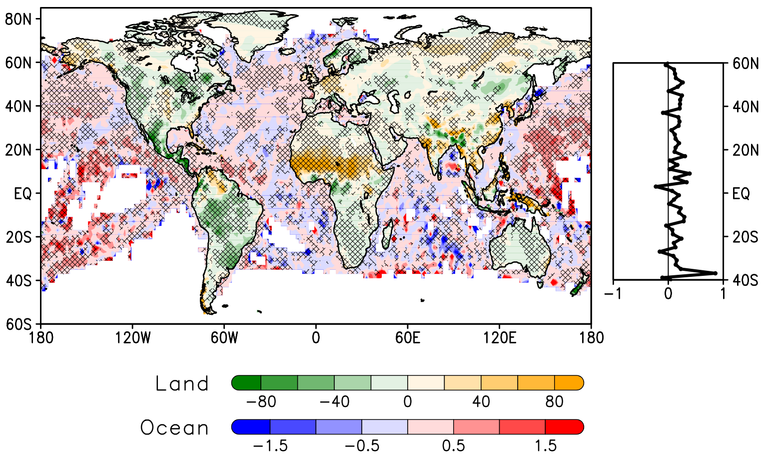

Figure 7. Left panel: trend shifts in the humidity deficit (g kg^{-1} 10 years^{-1}) over the ocean and right panel: latitude profile of its zonal mean. Land areas display trend shifts in JAS precipitation from Fig. 3a.

HESSD
12, 11269–11289, 2015

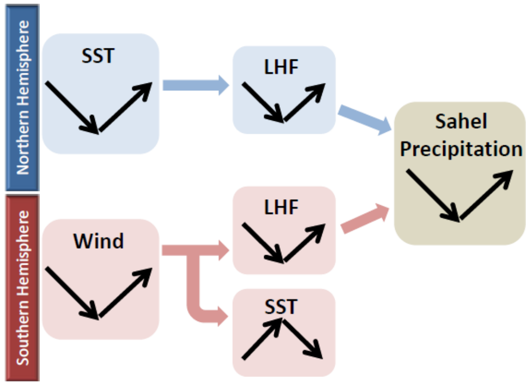

Figure 8. Schematic diagram of possible processes linking Sahel precipitation and the global ocean. The arrows represent increases or decreases in a parameter during 1950–1984 and 1985–2012.

HESSD
12, 11269–11289, 2015

Synchrony of trend shifts in Sahel summer rainfall and global oceanic evaporation

A. Diawara et al.

Title Page
Abstract Introduction
Conclusions References
Tables Figures
◀ ▶
Back Close
Full Screen / Esc
Printer-friendly Version
Interactive Discussion